Available online at www.sciencedirect.com
SCIENCE DIRECT
Journal of Photochemistry and Photobiology A: Chemistry 181 (2006) 283–289
Journal of Photochemistry and Photobiology A:Chemistry
www.elsevier.com/locate/jphotochem

Light-induced aggregation of cationic porphyrins

Jiří Mosinger[a,b,*], Martina Janošková[a], Kamil Lang[b], Pavel Kubát[c]

[a] *Faculty of Sciences, Charles University in Prague, 2030 Hlavova, 128 43 Prague 2, Czech Republic*
[b] *Institute of Inorganic Chemistry, Academy of Sciences of the Czech Republic, 250 68 Řež, Czech Republic*
[c] *J. Heyrovský Institute of Physical Chemistry, Academy of Sciences of the Czech Republic, Dolejškova 3, 182 23 Prague 8, Czech Republic*

Received 10 November 2005; received in revised form 6 December 2005; accepted 7 December 2005
Available online 18 January 2006

Abstract

The formation of ion-pairs between cationic porphyrins (5,10,15,20-tetrakis(*N*-methylpyridinium-4-yl)porphyrin (TMPyP), metallocomplexes Zn(II)TMPyP, Pd(II)TMPyP, Au(III)TMPyP, 5,10,15,20-tetrakis(α-[trimethylphosphonium]-*p*-tolyl)porphyrin, 5,10,15,20-tetrakis(α-pyridinio-*p*-tolyl)porphyrin) and triiodide anion leads to an extensive porphyrin aggregation in neutral aqueous solutions. Triiodide counteranion can be produced in situ by a photochemical reaction of cationic porphyrin sensitizers with oxygen in the presence of I^- since photoproduced singlet oxygen $^1O_2$ oxidizes I^- to I_3^-. The subsequent aggregation of the porphyrin/I_3^- ion-pairs causes fast quenching of the porphyrin triplet states and consequently restricts the formation of $^1O_2$. As a result, the formation of $^1O_2$ is stopped at a critical concentration of photoproduced triiodide. The presence of *calf thymus* DNA, cyclodextrin, or calixarene forming supramolecular assemblies with porphyrin and/or I_3^- prevents the formation of ion-pairs with I_3^- and preserves the effective production of $^1O_2$ by porphyrins. Aggregation is also eliminated at higher temperatures. Porphyrin Sn(IV)TMPyP does not aggregate probably because of two axial ligands and preserves its photosensitizing ability.

Keywords: Photosensitization; Singlet oxygen; Triiodide; Aggregation; Porphyrin

1. Introduction

Photosensitized reactions are implicated in many areas such as photodynamic therapy of cancer or atherosclerosis [1–3], photodynamic inactivation of pathogenic microorganisms [4], blood disinfection [5], degradation of polymers [6] and sun-light activated insecticides and pesticides [7]. The photodynamic effect rests in the oxidative damage of biological material by reactive forms of oxygen generated by sensitized reactions. The photodynamically active species is predominantly singlet oxygen $O_2(^1\Delta_g)$ generated in situ by energy transfer from an excited sensitizer to an oxygen molecule. Appropriate chemical and photophysical properties of a sensitizer such as spectral characteristics, fluorescence, photochemical stability and reasonable quantum yields of singlet oxygen formation Φ_Δ are prerequisites for effective photodynamic action. Some of water-soluble porphyrins are sensitizers with high Φ_Δ [8,9] having potential applications in biology and medicine [10]. The tendency of porphyrins to aggregate is not desirable since photodynamic efficiency decreases as a result of the poor or absent ability of dimer and higher aggregates to produce $^1O_2$ [11]. Binding of porphyrin sensitizers to biopolymers and/or transporting carriers is a subject of recent studies since the binding can cause changes of physico-chemical and photophysical properties and can avoid the aggregation [10,12].

Cationic porphyrins have attracted considerable attention as effective photodynamic sensitizers [13]. Due to their binding affinity towards nucleic acids, these porphyrins can selectively photocleave DNA [14,15], inhibit telomerases [16,17] and serve as vehicles for oligonucleotide delivery to tumors [18]. The photoinactivation of extremely resistant bacteria [19] and antiviral activity [20] were also reported. One of the most studied cationic porphyrin is 5,10,15,20-tetrakis(*N*-methylpyridinium-4-yl)porphyrin (TMPyP) (Scheme 1). Three binding modes have

Abbreviations: βCD, β-cyclodextrin; TMPyP, 5,10,15,20-tetrakis(*N*-methylpyridinium-4-yl)porphyrin; Zn(II)TMPyP, Zn(II) 5,10,15,20-tetrakis(*N*-methylpyridinium-4-yl)porphyrin; Pd(II)TMPyP, Pd(II) 5,10,15,20-tetrakis(*N*-methylpyridinium-4-yl)porphyrin; Au(III)TMPyP, Au(III) 5,10,15,20-tetrakis(*N*-methylpyridinium-4-yl)porphyrin; Sn(IV)TMPyP, Sn(IV) 5,10,15,20-tetrakis(*N*-methylpyridinium-4-yl)porphyrin; TPPS, 5,10,15,20-tetrakis(4-sulfonatophenyl)porphyrin; TTPP, 5,10,15,20-tetrakis(α-[trimethylphosphonium]-*p*-tolyl)porphyrin; TTPPy, 5,10,15,20-tetrakis(α-pyridinio-*p*-tolyl)porphyrin

* Corresponding author. Tel.: +420 221 951 255; fax: +420 221 951 253.
E-mail address: mosinger@natur.cuni.cz (J. Mosinger).

1010-6030/$ – see front matter © 2005 Elsevier B.V. All rights reserved.
doi:10.1016/j.jphotochem.2005.12.009

been described for the interaction of TMPyP with DNA: (i) intercalation, (ii) outside groove binding, and (iii) outside binding with porphyrin self-stacking [21–23]. External binding and ion-pairing was observed for interaction with cyclodextrins and calixarenes, respectively [10,24].

Recently, the important role of counteranions was reported in acid-induced aggregation of tetrapyridylporphyrins in organic solvents. The protonated species and resulting aggregates exhibit spectroscopic features that are markedly influences by nature of the counteranions [25]. In contrast to other cationic porphyrins TMPyP is reported to be monomeric in organic and aqueous solutions over the extended concentration range ($<10^{-4}$ M) even at high ionic strength as shown by detailed UV–vis, fluorescence and NMR experiments [26–29]. As proposed the delocalized positive charges on the porphyrin periphery are responsible for electrostatic repulsion between the porphyrin units. The repulsion forces hinder the formation of dimers and higher aggregates. Herein we report aggregation behavior of seven cationic porphyrin and metalloporphyrin sensitizers including TMPyP induced by photogenerated I_3^- via oxidation of I^- by photosensitized $^1O_2$ in aqueous solutions. We also demonstrate the consequence of light-induced aggregation on photochemical behavior of porphyrins. In addition we show the importance of a carrier/target on the monomerization of cationic porphyrins and production of $^1O_2$.

2. Experimental details

2.1. Chemicals

A tetratosylate salt of TMPyP, β-cyclodextrin (βCD), *calf thymus* DNA (all from Fluka), Zn(II)TMPyP tetrachloride, Pd(II)TMPyP tetrachloride, Au(III)TMPyP pentachloride and Sn(IV)TMPyP hexachloride (all Porphyrin Systems), iodide and other inorganic salts (all Aldrich) were used as received (Scheme 1). The synthesis and characterization of 5,10,15,20-tetrakis(4-sulfonatophenyl)porphyrin (TPPS) [30], 5,10,15,20-tetrakis(α-[trimethylphosphonium]-*p*-tolyl)porphyrin tetrabromide salt (TTPP) and 5,10,15,20-tetrakis(α-pyridinio-*p*-tolyl)porphyrin tetrabromide salt (TTPPy) [31,32] were presented elsewhere (Scheme 1). Calix[4]arene-*p*-tetrasulfonate was synthesized by direct sulfonation of calix[4]arene and purified [33]. Aqueous solutions of I_3^- were prepared by mixing

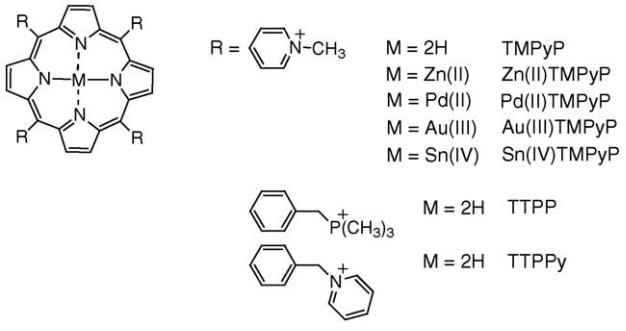

Scheme 1. Molecular structures of studied porphyrins.

I_2 and KI solutions keeping the concentration of KI at least at 100 mol excess. All solutions of I_2, I^- and I_3^- were kept in darkness.

2.2. Methods

The UV–vis absorption spectra were measured on a Unicam 340 and on a Varian Cary IE spectrophotometer using 10 or 1 mm quartz cells. Resonance light-scattering (RLS) experiments were performed on a Perkin-Elmer LS 50B luminescence spectrometer using simultaneous scans of excitation and emission monochromators ranging from 300–700 nm. Laser flash photolysis experiments were performed with a Lambda Physik FL 3002 dye laser (417 nm, output energy 1–3 mJ/pulse, pulse width ~28 ns). The time profiles of the porphyrin triplet states were probed at 460 nm using a 250 W Xe lamp equipped with a pulse unit and a R928 photomultiplier. All experiments were performed in deionized water at 22 °C unless otherwise stated.

The singlet oxygen formation was followed using the iodide method [34,35]. The amount of photoproduced I_3^- is directly proportional to the concentration of $^1O_2$ that is produced during continuous irradiation. Two milliliters of a detection solution (0.1 M KI, 10 μM $(NH_4)_2MoO_4$, 0.02 M phosphate buffer, pH 6.2) containing porphyrin were placed into a thermostatted 10 mm quartz cell (22 °C) and irradiated by a 5 mW He–Ne laser (543 nm) or by a 300 W stabilized halogen lamp. The solution was stirred during irradiation. The absorbance at the excitation wavelength of 543 nm was kept below 0.1 to eliminate inner filter effects due to self-absorption of light by porphyrins. The increasing absorbance of the I_3^- band was recorded at 351 nm and compared with a blank solution of the same composition kept in the dark.

3. Results and discussion

3.1. Aggregation in aqueous solutions

The solutions of TMPyP were investigated up to 1×10^{-4} M in the absence and presence of 0.1 M KF, KCl, KBr and KNO_3 to increase ionic strength. No changes of the absorption and fluorescence spectra of TMPyP were observed. Thus, our experiments confirmed that TMPyP remains monomeric in aqueous solutions [26–29]. Surprisingly, considerable hypochromicity and broadening of the porphyrin Soret band, increased turbidity and deviations from the linearity of the Lambert–Beer plots are observed in the presence of 0.1 M KI after the solution is exposed to the daylight while no changes proceed in the dark. Since TMPyP is an sensitizer producing $^1O_2$ with quantum yields Φ_Δ ranging from 0.58 to 0.9 [9,36,37], all other experiments were performed under controlled irradiation conditions and concentration of dissolved oxygen. In an oxygen-free solution the hypochromicity does not appear (Fig. 1a), however, it is immediately induced after admitting oxygen as shown by decreasing absorption of the TMPyP Soret band at 422 nm ($\varepsilon_{422} = 2.2 \times 10^5$ M^{-1} cm^{-1} in the monomer state) (Fig. 1b). To summarize, the described spectral changes occur only in the simultaneous presence of KI, oxygen and light.

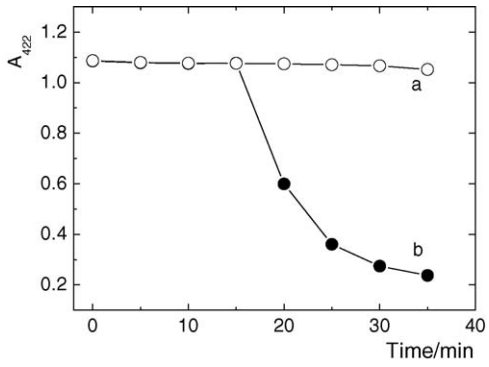

Fig. 1. Absorbance changes of 5×10^{-6} M TMPyP in 0.1 M KI recorded at 422 nm in the absence of oxygen (a) and after saturation by air (b) during continuous irradiation by a 5 mW He–Ne laser.

Beside TMPyP we tested corresponding metalloporphyrins Zn(II)TMPyP, Pd(II)TMPyP, Au(III)TMPyP, Sn(IV)TMPyP and other cationic porphyrins TTPP and TTPPy (Scheme 1). Except for Sn(IV)TMPyP all studied cationic porphyrins exhibit above described spectral changes.

3.2. Mechanism of self-aggregation

In general, aggregation of cationic porphyrins is accompanied by spectral changes in their absorption and fluorescence spectra. The Soret bands of face-to-face (H-type) and edge-to-edge (J-type) aggregates are blue-shifted and red-shifted, respectively [26,38–40]. In the presented case a considerable broadening of the absorption bands with no characteristic spectral features and diminishing intensity of the emission spectra indicate nonspecific aggregates. Nonspecific aggregates are formed by more hydrophobic tetrapyridinium porphyrins [26] and in the case of TMPyP by surfactant-induced effects [39]. Our findings can be explained by extensive porphyrin aggregation occurring under irradiation of air-saturated aqueous solutions in the presence of I^-. No iodide-induced aggregation of cationic porphyrins has been reported so far.

Continuous irradiation of porphyrin air-saturated solutions in the presence of I^- leads to the increasing concentration of photoproduced I_3^- having the absorption bands at 287 and 351 nm (Figs. 2 and 3B). Generation of certain concentration of I_3^- (Fig. 3B-a) is accompanied by a remarkable hypochromicity of the Soret band (Fig. 3A-b) and increased background due to light scattering on aggregate particles indicating a close relationship between I_3^- and porphyrin aggregation (Fig. 2A and B). The formation of extended electronically coupled aggregates during irradiation was also evidenced using RLS experiments. This technique allows identification of extended aggregate species even at low concentrations since the amount of scattered light is directly proportional to the volume of particles and monomeric molecules and small oligomers show no enhanced scattering [26,41]. The RLS spectra shown in Fig. 2A and B (insets) reveal broad peaks at 520 nm. It indicates that the size of aggregates is large enough to scatter light and a presumable contribution of J-aggregate structures. In the absence of light and/or dissolved oxygen, I_3^- is not produced and aggregation does not occur

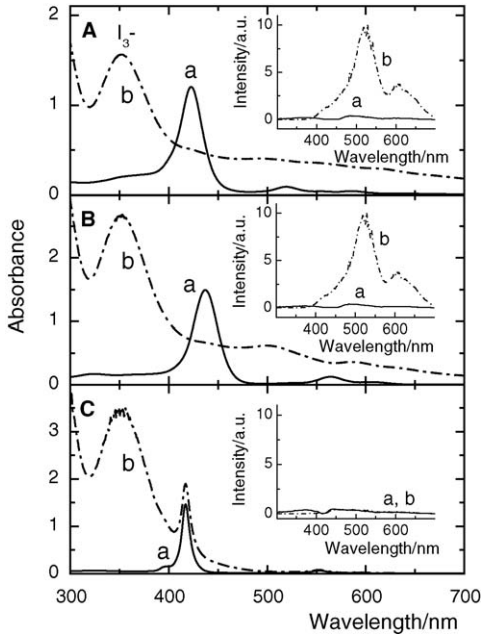

Fig. 2. UV–vis spectra of air-saturated porphyrin solutions in the presence of 0.1 M KI before (a) and after 2 min irradiation by a 300 W halogen lamp (b): (A) 5×10^{-6} M TMPyP; (B) 8×10^{-6} M ZnTMPyP; (C) 4×10^{-6} M SnTMPyP; insets: corresponding RLS spectra.

signifying again the important role of I_3^- for the aggregation process.

On the contrary, photoproduction of I_3^- by Sn(IV)TMPyP has no effect on the molecular state as documented by UV–vis

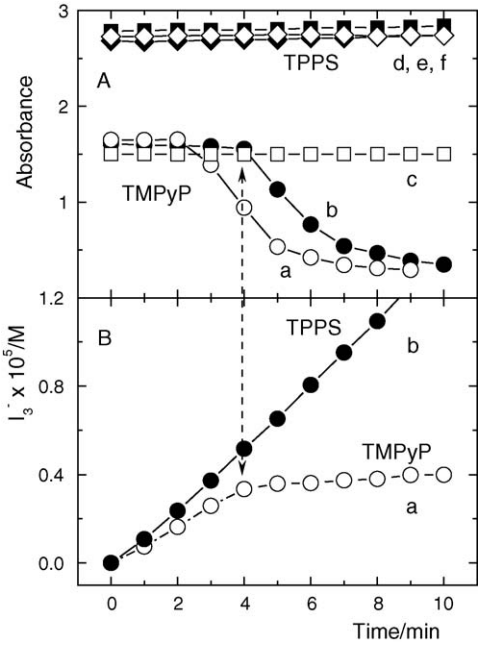

Fig. 3. (A) Absorption changes of the Soret bands during irradiation by a 5 mW He–Ne laser: 7×10^{-6} M TMPyP recorded at 422 nm in D_2O (a), H_2O (b) and in H_2O in the presence of 0.1 M NaN_3 (c), 7×10^{-6} M TPPS recorded at 412 nm in D_2O (d), H_2O (e) and in H_2O in the presence of 0.1 M NaN_3 (f). (B) Concentration of I_3^- produced by irradiation of optically matched solutions ($A_{543\,nm} = 0.1$) of TMPyP (a) and TPPS (b) in air-saturated 0.02 M phosphate buffer, pH 6.2, 0.1 M KI, 10 μM $(NH_4)_2MoO_4$.

and RLS spectra (Fig. 2C). The absorption spectra of I_3^- and Sn(IV)TMPyP overlap with no indication of any spectral changes ascribed to aggregation. The observed minimum at 420 nm in RLS (Fig. 2C, inset) is due to self-absorption. The results confirm that Sn(IV)TMPyP remains monomeric. Most probably two axial ligands on the central atom hinder the aggregation process.

Triiodide I_3^- is produced by photooxidation of I^- by $^1O_2$ [42]:

$$\text{Porph} + h\nu \rightarrow {}^1\text{Porph} \rightarrow {}^3\text{Porph}$$

(excitation, intersystem crossing) (1)

$${}^3\text{Porph} + {}^3O_2 \rightarrow \text{Porph} + O_2({}^1\Delta_g)$$

(energy transfer to oxygen) (2)

$$^1O_2 + I^- + H_2O \underset{-OH^-}{\longrightarrow} IOOH \xrightarrow{I^-} I_2 + HO_2^-$$

$$\xrightarrow{I^-,H_2O} I_3^- + H_2O_2 + OH^- \quad (3)$$

$$H_2O_2 + 2I^- + 2H^+ \underset{-2H_2O}{\longrightarrow} I_2 \xrightarrow{I^-} I_3^- \quad (4)$$

The importance of $^1O_2$ for the formation of I_3^- and consequently for porphyrin aggregation was further tested in D_2O and using singlet oxygen quencher NaN_3. A marked acceleration of the formation of I_3^- and aggregation of TMPyP (Fig. 3A-a and b) fully corresponds to a higher efficiency of $^1O_2$ to oxidize I^- to I_3^- in D_2O since the lifetime of $^1O_2$ is much longer in D_2O (~60 μs) than in H_2O (~4 μs) [43]. In air-saturated solution containing NaN_3, no production of I_3^- and no porphyrin aggregation were observed (Fig. 3A-c) since NaN_3 efficiently quenches $^1O_2$ [43]. No aggregation or photobleaching of TPPS proceeds under the same conditions (Fig. 3A-d–f) signifying the importance of the charge on the porphyrin periphery.

The concentration of photoproduced I_3^- is proportional to the sensitized concentration of $^1O_2$ [34,35]. This is documented by linear increase of the concentration of I_3^- produced by TPPS during continuous irradiation (Fig. 3B-b). There is no indication of aggregation or photobleaching of TPPS. On the contrary, during irradiation of an optically matched solution of TMPyP the formation rate of I_3^- slows down as the aggregation process proceeds (cf. Fig. 3A-b and B-a). Finally, the concentration of I_3^- reaches a constant value. It indicates that the formation of $^1O_2$ stops at a critical concentration of I_3^- causing the complete aggregation of TMPyP.

The behavior of the porphyrin triplet states was verified using time-resolved transient spectroscopy (Fig. 4). The triplet states of TMPyP (Fig. 4a, oxygen-free solution) are quenched by oxygen to form $^1O_2$ (Eq. (2)) as documented by the trace in Fig. 4b. The triplet states are competitively quenched by I^- itself (cf. Fig. 4b and c), however, the presence of I^- does not stop quenching by oxygen, the formation of $^1O_2$ and consequently oxidation of I^- to I_3^- (Figs. 2 and 3). In contrast, porphyrin triiodide aggregates do not have long-living triplet states due to fast dissipation of absorbed energy and, therefore, no $^1O_2$ is formed (Fig. 4d).

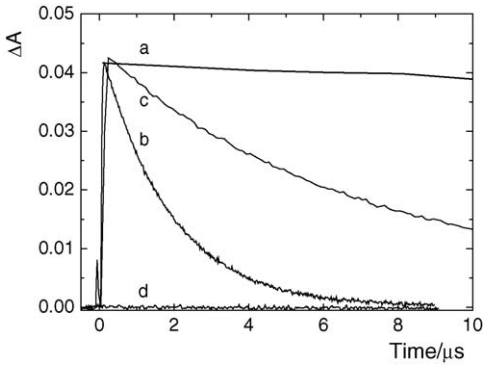

Fig. 4. Quenching of the triplet states of TMPyP recorded in oxygen-free water (a) by oxygen (b, air-saturated) and by 1×10^{-3} M I^- (c). Trace (d) belongs to aggregates formed by the addition of 2.5×10^{-4} M I_3^-/0.1 M KI to a TMPyP solution in air-saturated water. The concentration of TMPyP was 4×10^{-6} M.

In water TMPyP photobleaches using a high fluence rate of 150 mW/cm^2 [44]. In contrast, photobleaching of porphyrins in our experiments can be excluded. (i) In a typical experiment solutions were irradiated by low intensity light. No spectral changes were observed in the absence of oxygen and iodide indicating that porphyrins are photostable under our irradiation conditions. (ii) Photobleaching via the singlet oxygen route can be excluded as no spectral changes are observed in the only presence of oxygen. Similarly, iodide itself does not photobleach studied porphyrins. In the presence of both iodide and oxygen produced $^1O_2$ interacts predominantly with I^- since its concentration is much higher than that of porphyrins (e.g. 10^{-1} to 10^{-4} M I^- versus 2–8 $\times 10^{-6}$ M porphyrin). (iii) In most cases photobleaching reactions are irreversible; however, the presented spectral changes are fully reversible as documented in Section 3.3.

The effect of I_3^- on porphyrin aggregation was further confirmed by adding aliquots of a I_3^- solution. Immediate aggregation of TMPyP occurs (Fig. 5A-b). The appearance of broad RLS features in Fig. 5A-g clearly shows the contribution of extended aggregates. At larger concentrations of TMPyP (above 10^{-5} M), aggregation is followed by the instant formation of a dark brown voluminous precipitate. Aggregation is reversible since upon heating a solution the spectral features of monomeric porphyrin reappears (Fig. 5A-a) (see Section 3.3). Similar behavior was observed for all tested porphyrins except for Sn(IV)TMPyP (Fig. 5B).

The exposure of a TMPyP solution to iodine vapors induces fast aggregation/precipitation only in the presence of KI (Fig. 6A). The band of I_3^- is generated, the Soret band of TMPyP practically disappears and the spectral background increases as a result of an increased scattering on aggregate particles. In the absence of KI, only a slight aggregation occurs as the disproportionation reaction of iodine to I^- is a slow process (Fig. 6B). These results again confirm that the observed aggregation process occurs only when I_3^- is photoproduced or added to a solution.

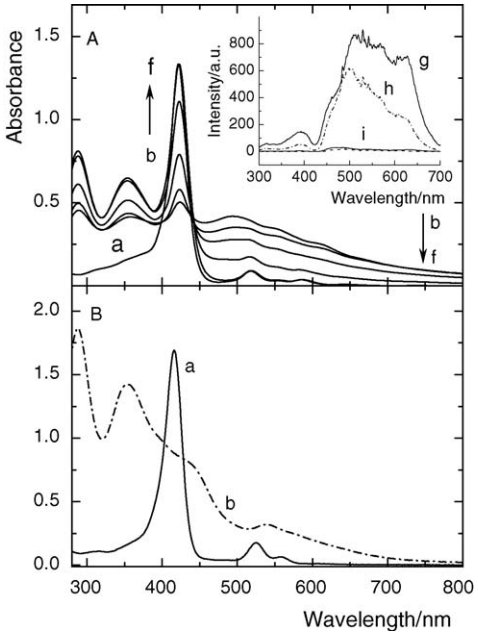

Fig. 5. (A) Absorption spectra of 6×10^{-6} M TMPyP in H_2O (a) and after addition of 2.4×10^{-5} M I_3^-/0.1 M KI at 10, 20, 30, 40, 60 °C (b–f). Inset: corresponding RLS spectra at 23 °C (g), 40 °C (h) and 60 °C (i). (B) Absorption spectra of 1×10^{-5} M Pd(II)TMyP before (a) and after addition of 2.4×10^{-5} M I_3^-/0.1 M KI (b) at 22 °C.

Titration curves were constructed by adding I_3^- to a TMPyP solution whose concentration was kept constant. Using micromolar concentrations of TMPyP titrations reveal that the overall stoichiometry between TMPyP and I_3^- is 1:4 (Fig. 7). The same stoichiometry was also determined by elemental analysis of the voluminous precipitate obtained by adding large excess of I_3^-. The observations suggest ion-pairing between TMPyP and I_3^-. Four positive charges located on the porphyrin periphery inter-

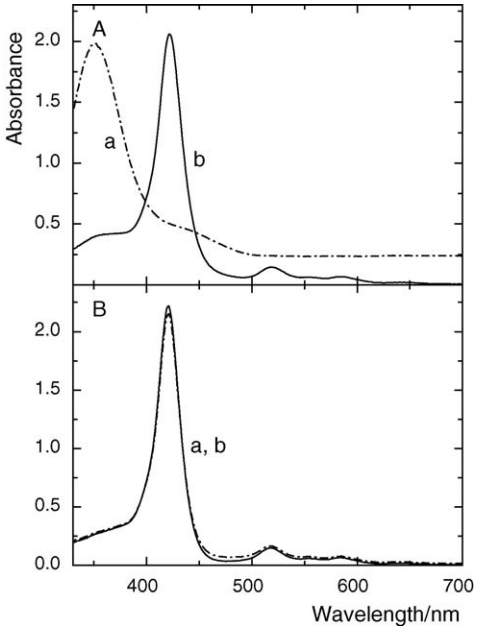

Fig. 6. Absorption spectra of 10^{-5} M TMPyP in H_2O in the presence (A) and absence (B) of 0.03 M KI before (b) and after (a) exposure to iodine vapors.

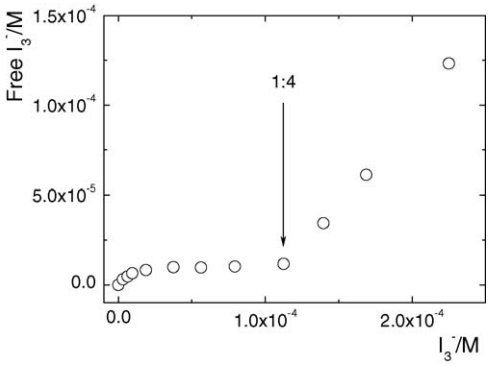

Fig. 7. Titration of 2.8×10^{-5} M TMPyP by I_3^- in 0.1 M KI. After reaching 1.1×10^{-4} M I_3^- the concentration of free (unbound) I_3^- grows linearly. Arrow indicates the stoichiometry of TMPyP/I_3^-.

act with four I_3^- leading to the uncharged nonpolar species (Eq. (5)). Titrations of higher concentrations of TMPyP (10^{-4} M, 22 °C) also indicate the consecutive stoichiometries 1:1 and 1:2:

$$\text{TMPyP} + 4I_3^- \rightleftarrows \text{TMPyP-}(I_3^-)_4 \quad \text{(aggregation/precipitation)} \tag{5}$$

Aggregation induced by I_3^- is not only limited to TMPyP. Except for Sn(IV)TMPyP all other tested metalloporphyrins Zn(II)TMPyP, Pd(II)TMPyP, Au(III)TMPyP aggregate. Porphyrins TTPP and TTPPy have positively charged substituents separated from the porphyrin ring by the methylene spacers, preventing the delocalization of the positive charge within the tetraphenylporphyrin π-electron system by a direct coupling. The photophysical properties are similar to those of TMPyP, however, these porphyrins are more prone to self-aggregate [38]. Similarly to TMPyP, photoproduction of I_3^- leads to the extended aggregation of TTPP and TTPPy. These results document that triiodide-induced aggregation is not affected by the localization of the positive charges.

The cationic porphyrin/I^- systems are effective sensitizers of $^1O_2$ losing their sensitizing ability during irradiation. The compensation of the positive charges by the large lipophilic, easily polarizable I_3^-, in contrast to other loosely bound counterions, compensates electrostatic repulsion between neighboring porphyrin units and causes low solubility of the uncharged ion-pairs. The importance of ion-pairing is confirmed by experiments with TPPS having four peripheral anionic sulfonates. Electrostatic repulsion between sulfonates and I_3^- does not allow aggregation (Fig. 3).

3.3. Factors influencing self-aggregation

Based on detailed result analysis the extent of aggregation depends on the following factors.

3.3.1. Temperature

Aggregate structures can be monomerized at higher temperatures [38]. Similarly, the Soret band of TMPyP reappears after heating a solution of porphyrin/I_3^- aggregates to 60 ± 2 °C (Fig. 5A). The appearance of monomeric TMPyP is accompa-

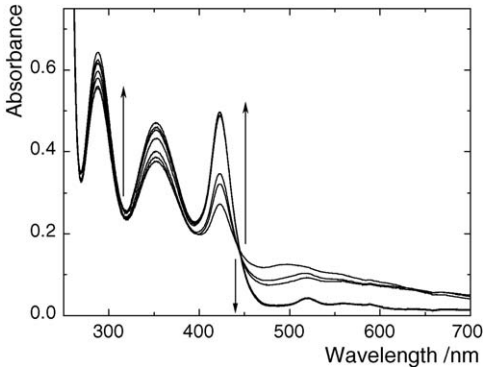

Fig. 8. Deaggregation of porphyrin/I_3^- aggregates (2×10^{-6} M TMPyP/1.7×10^{-5} M I_3^-/0.1 M KI) using 0–0.5 M KCl at room temperature. Arrows show spectral changes with increasing concentration of KCl.

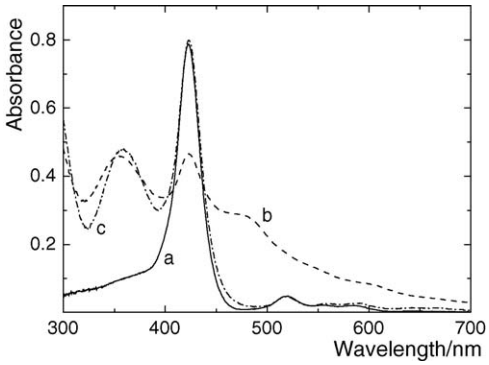

Fig. 9. Absorption spectra of 4×10^{-6} M TMPyP (a), after the addition of 1.7×10^{-5} M I_3^-/0.1 M KI (b), and after subsequent addition of 4×10^{-4} M βCD (c). 0.02 M phosphate buffer, pH 7.0.

nied by growing concentration of free I_3^- (absorption bands at 287 and 351 nm). After cooled to laboratory temperature aggregation again proceeds. Aggregation/deaggregation cycles can be repeated with no indication of any porphyrin degradation. Lower extent of aggregation at elevated temperatures is confirmed by RLS by decreasing intensity of scattered light (Fig. 5A, inset). At 60 °C no enhanced scattering is observed, which is consistent with the fact that only the monomer is present.

3.3.2. Concentration, time and pH

Higher concentrations of porphyrins or I^- (i.e. of photoproduced I_3^-) increase the extent of aggregation. Aggregation is a time-dependent process and its extent increases in time. The amount of aggregates rapidly drops at pH below 1.4, the value matching pK_a of TMPyP. It implicates that protonation of the porphyrin ring prevents the formation of aggregates due to increased electrostatic repulsion between the porphyrin units.

3.3.3. Indifferent ions

The excess of indifferent ions prevents aggregation/precipitation of porphyrins. This is an opposite effect than expected since water-soluble porphyrins aggregate at increased ionic strength [10,31,38]. As an example, no aggregation occurs in a solution containing TMPyP, I_3^- and 0.5 M KCl (Fig. 8). If the concentration of Cl^- is comparable to that of I_3^- substantial aggregation takes place. Evidently, the competition between counteranions I_3^- and Cl^- is responsible for porphyrin monomerization.

3.3.4. Solvent

Aggregation occurs in aqueous solutions. The addition of methanol or ethanol up to 60% v/v leads to a gradual monomerization of aggregates.

3.3.5. Competitive binding

To obtain an idea how to control aggregation and consequently the photophysical properties of studied porphyrins, the UV–vis and fluorescence features were examined in the presence of macrocyclic compounds having an internal cavity such as βCD and calix[4]arene-*p*-tetrasulfonate, and biopolymers, such as *calf thymus* DNA. Cyclodextrin βCD forms inclusion complexes with I_3^- [45] and anionic porphyrins [46] while cationic TMPyP is bound to the cyclodextrin external surface [10]. Fig. 9 illustrates the effect of βCD on the absorption spectrum of TMPyP/I_3^- aggregates. The addition of βCD resulted in an enhancement of the porphyrin monomer absorbance and a bathochromic shift of the I_3^- band from 351 to 359 nm indicating the inclusion of I_3^- into the cyclodextrin cavity (Fig. 9b and c). Thus, I_3^- is encapsulated in the βCD cavity and TMPyP does not aggregate (Fig. 9a and c). As a result, the photosensitizing properties of TMPyP are restored to the original characteristics. Triiodide aggregates of other studied porphyrins behave similarly. Since calix[4]arene-*p*-tetrasulfonate forms a 1:1 complex with TMPyP, the porphyrin and I_3^- are separated each other and no aggregation occurs. In this case, however, the photophysical properties of the TMPyP-calix[4]arene-*p*-tetrasulfonate complex differ from those of TMPyP [24].

The addition of DNA also causes monomerization of TMPyP/I_3^- aggregates (Fig. 10). Aggregates can be removed by centrifugation giving the neat spectrum of free I_3^- (Fig. 10c). DNA has a strong monomerization effect and I_3^- captured within aggregate species is released to a solution (Fig. 10d). The red shift of the TMPyP Soret band from 422 to 436 nm (Fig. 10a and d) indicates binding of TMPyP to double stranded

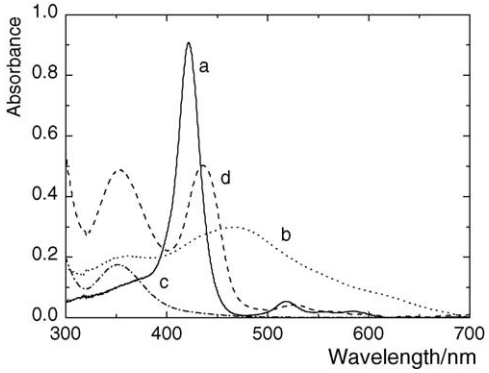

Fig. 10. Absorption spectra of 4×10^{-6} M TMPyP in the absence (a) and presence of 8×10^{-4} M I_3^- (b). The same solution after centrifugation (c) and after subsequent addition of 3.4×10^{-5} M *calf thymus* DNA (d). 0.02 M phosphate buffer, pH 7.0.

DNA as TMPyP intercalates predominantly at GC base pairs and is bound in grooves at AT base pair rich sequences [21–23].

The presented results reveal that monomerization of cationic porphyrins can be achieved by the addition of competitive binders such as cyclodextrin, calix[4]arene and nucleic acids. These non-covalent interactions affect a photosensitized concentration of $^1O_2$ and all processes that involve $^1O_2$.

4. Conclusion

The studied cationic porphyrin sensitizers bearing pyridinium or phosphonium groups on the periphery are predominantly monomeric in aqueous solutions. However, in the simultaneous presence of iodide, oxygen and light the extensive aggregation occurs. The aggregation is mediated by photogenerated counteranion I_3^-, which is produced by oxidation of I^- by $^1O_2$ photosensitized by porphyrins. Since the triplet states within aggregates are quenched by fast relaxation processes, no $^1O_2$ is produced after reaching a critical concentration of I_3^-. In other words, we present a switch-off photochemical reaction that can be utilized in porphyrin aggregation/deaggregation processes and in applications requiring $^1O_2$. We also demonstrate the importance of the shielding effect of molecular carriers against aggregation of cationic sensitizers in an environment causing aggregation/photoaggregation. The molecular carriers, such as cyclodextrin or calixarene, form non-covalent supramolecular complexes with porphyrins and/or I_3^- causing the monomerization/solubilization of the aggregate and keeping the production of $^1O_2$ effective. Induced aggregation by photochemically formed I_3^- and backward deaggregation/solubilization influences all processes involving singlet oxygen.

Acknowledgments

This work was supported by the Czech Science Foundation (Grant Nos. 203/02/0420, 203/02/1483 and 203/04/0426). The authors wish to thank P. Anzenbacher Jr. of the Bowling Green State University, OH, USA for the samples of TTPP and TTPPy, and P. Lhoták of the Institute of Chemical Technology, Prague for the sample of calix[4]arene-*p*-tetrasulfonate.

References

[1] I.J. MacDonald, T.J. Dougherty, J. Porphyrins Phthalocyanines 5 (2001) 105–129.
[2] E.S. Nyman, P.H. Hynninen, J. Photochem. Photobiol. B 73 (2004) 1–28.
[3] Y.N. Hsiang, M.T. Crespo, A.M. Richter, A.K. Jain, M. Fragoso, J.G. Levy, Photochem. Photobiol. 54 (1993) 670–674.
[4] M.R. Hamblin, T. Hasan, Photochem. Photobiol. Sci. 3 (2004) 436–450.
[5] M. Wainwright, Chem. Soc. Rev. 31 (2002) 128–136.
[6] C. Tanielian, R. Mechin, M. Shakirullah, J. Photochem. Photobiol. A 64 (1992) 191–199.
[7] T. Ben-Amor, G. Jori, Insect Biochem. Mol. Biol. 30 (2000) 915–925.
[8] R.W. Redmond, J.N. Gamlin, Photochem. Photobiol. 70 (1999) 391–475.
[9] F. Wilkinson, W.P. Helman, A.B. Ross, J. Phys. Chem. Ref. Data 22 (1993) 113–262.
[10] K. Lang, J. Mosinger, D.M. Wagnerová, Chem. Rev. 248 (2004) 321–350.
[11] F. Ricchelli, J. Photochem. Photobiol. B: Biol. 29 (1995) 109–118.
[12] J. Mosinger, M. Deumié, K. Lang, P. Kubát, D.M. Wagnerová, J. Photochem. Photobiol. A 130 (2000) 13–20.
[13] R.W. Boyle, D. Dolphin, Photochem. Photobiol. 64 (1996) 469–485.
[14] B. Armitage, Chem. Rev. 98 (1998) 1171–1200.
[15] S. Mettath, B.R. Munson, R.K. Pandey, Bioconjugate Chem. 10 (1999) 94–102.
[16] I. Haq, J.O. Trent, B.Z. Chowdhry, T.C. Jenkins, J. Am. Chem. Soc. 121 (1999) 1768–1779.
[17] F.X. Han, R.T. Wheelhouse, L.H. Hurley, J. Am. Chem. Soc. 121 (1999) 3561–3570.
[18] C.R. Dass, J. Pharm. Pharmacol. 54 (2002) 3–27.
[19] Y. Nitzan, H. Ashkenazi, Photochem. Photobiol. 69 (1999) 505–510.
[20] A.K. Debnath, S. Jiang, N. Strick, P. Haberfield, R.A. Neurath, J. Med. Chem. 37 (1994) 1099–1108.
[21] R.J. Fiel, J. Biomol. Struct. Dynam. 6 (1989) 1259–1274.
[22] R.F. Pasternack, E.J. Gibs, J.J. Villafranca, Biochemistry 22 (1983) 2406–2414.
[23] P. Lugo-Ponce, D.R. McMillin, Coord. Chem. Rev. 208 (2000) 169–191.
[24] K. Lang, P. Kubát, P. Lhoták, J. Mosinger, D.M. Wagnerová, Photochem. Photobiol. 74 (2001) 558–565.
[25] G. De Luca, A. Romeo, L.M. Scolaro, J. Phys. Chem. B 109 (2005) 7149–7158.
[26] K. Kano, K. Fukuda, H. Wakami, R. Nishiyabu, R.F. Pasternack, J. Am. Chem. Soc. 122 (2000) 7494–7502.
[27] F.J. Vergeldt, R.B.M. Koehorst, A. van Hoek, T.J. Schaafsma, J. Phys. Chem. 99 (1995) 4397–4405.
[28] D.L. Akins, H.R. Zhu, C. Guo, J. Phys. Chem. 100 (1996) 5420–5425.
[29] K. Kano, H. Minamizano, T. Kitae, S. Negi, J. Phys. Chem. 101 (1997) 6118–6124.
[30] P. Kubát, J. Mosinger, J. Photochem. Photobiol. A 96 (1996) 93–97.
[31] P. Kubát, K. Lang, V. Král, P. Anzenbacher, J. Phys. Chem. B 106 (2002) 6784–6792.
[32] P. Kubát, K. Lang, P. Anzenbacher, K. Jursíková, V. Král, B. Ehrenberg, J. Chem. Soc., Perkin Trans. 1 (2000) 933–941.
[33] S. Shinkai, K. Araki, T. Tsubaki, T. Arimura, O. Manabe, J. Chem. Soc., Perkin Trans. 1 (1987) 2297–2299.
[34] J. Mosinger, B. Mosinger, Experientia 51 (1995) 106–109.
[35] J. Mosinger, Z. Micka, J. Photochem. Photobiol. A 107 (1997) 77–82.
[36] N.N. Kruk, B.M. Dzhagarov, V.A. Galievsky, V.S. Chirvony, P.Y. Turpin, J. Photochem. Photobiol. B 42 (1998) 181–190.
[37] T. Gensch, C. Viappiani, S.E. Braslavsky, J. Am. Chem. Soc. 121 (1999) 10573–10582.
[38] P. Kubát, K. Lang, K. Procházková, P. Anzenbacher, Langmuir 19 (2003) 422–428.
[39] N.C. Maiti, S. Mazumdar, N. Periasami, J. Phys. Chem. B 102 (1998) 1528–1538.
[40] K. Procházková, Z. Zelinger, K. Lang, P. Kubát, J. Phys. Org. Chem. 17 (2004) 890–897.
[41] P.J. Collings, E.J. Gibbs, T.E. Starr, O. Vafek, C. Yee, L.A. Pomerance, R.F. Pasternack, J. Phys. Chem. B 103 (1999) 8474–8481.
[42] G. Braathen, P.T. Chou, H. Frei, J. Phys. Chem. 92 (1988) 6610–6615.
[43] F. Wilkinson, W.P. Helman, A.B. Ross, J. Phys. Chem. Ref. Data 24 (1995) 663–1021.
[44] E. Reddi, M. Ceccon, G. Valduga, G. Jori, J.C. Bommer, F. Elisei, L. Latterini, U. Mazzucato, Photochem. Photobiol. 75 (2002) 462–470.
[45] J.P. Diard, E. Saint-Aman, D. Serve, J. Electroanal. Chem. 189 (1985) 113–120.
[46] K. Kano, R. Nishiyabu, T. Asada, Y. Kuroda, J. Am. Chem. Soc. 124 (2002) 9937–9944.